International Journal of Environmental Science and Technology
https://doi.org/10.1007/s13762-025-06673-1

ORIGINAL PAPER

# Impact of different air flow rates on disinfection efficacy of multi lamp in-duct UVC air disinfection system

**M. P. Sharma**[1] · **A. Ahmadian**[2,3]

Received: 5 January 2025 / Revised: 4 June 2025 / Accepted: 12 July 2025


## Abstract

Highly consequential healthcare-associated infections stem from multidrug-resistant (MDR) pathogens, culminating in escalated morbidity and mortality rates. In combating airborne MDR pathogens, in-duct Ultraviolet-C technology emerges as a viable solution, necessitating systematic enhancement of its disinfection efficacy and performance. By employing computational fluid dynamics (CFD), we fortify the efficacy and performance of a 13-lamp configured in-duct air disinfection system. The Discrete Ordinates method (DO) and user-defined function (UDF) have been used for modeling lamp irradiation and finding the average Ultraviolet-C dose of the system. In this paper, the impact of different input air flow rates on the disinfection efficacy and type of airflow inside the in-duct Ultraviolet-C air disinfection system has been studied. It has been found from this study that particles having longest resident time are aligned among particles with the lowest Ultraviolet-C dose obtained. When air velocity is increased, Ultraviolet-C dose that every particle received changes in magnitude. At high velocity the particles experienced less Ultraviolet-C dose and vice versa. The Ultraviolet-C dose distribution, however, remains relatively consistent while rate of air flow changes. The derived performance efficiency rating (PER) of 0.94 gauges the system's efficacy; notably, this surpasses EPA test series ratings by more than 50%. Turbulence analysis demonstrates that airflow within the duct is not fully turbulent, indicating no direct turbulence-UV dose relationship. However, airflow patterns within the duct markedly impact system sterilization efficacy.

**Keywords** Computational fluid dynamics (CFD) · Discrete ordinate method (DO) · Performance efficiency rating (PER) · Ultraviolet-C · User-defined function (UDF)

## Introduction

By eliminating or inactivating the pollutants and pathogenic microorganisms that are present in the environment, clean air technologies improve the indoor air quality. In recent years, rapid spread of infectious diseases has accentuated the need for advanced infection control strategies. Ultraviolet-C (UVC) disinfection systems have emerged as a promising solution, harnessing the power of UVC radiation to neutralize pathogens. "Such disinfection devices may work more efficiently than conventional filters due to their capacity to destroy or decompose pathogens genetic material" (Blatt 2006; Kowalski 2009; Lee et al. 2009; Luckiesh 1946). UVC radiation inactivates microorganisms by creating thymine dimers in their DNA that alter the replication process and stop any further infections. Several previously published studies showed that at 254 nm wavelength UVC successfully deactivated several airborne pathogens, including some multidrug-resistant (MDR) bacteria and viruses. Apart from its germicidal property, UVC is also utilized in air disinfection systems due to the fact that it can pass through the ventilation ducts and neutralize pathogens in the air streams. This research looks at the efficacy of an in-duct, multi-lamp UVC-air disinfection system and quantifies how different values of airflow rates affect UVC dose distribution. "The UVC radiations sterilization ability has been demonstrated

Editorial responsibility: Samareh Mirkia.

✉ A. Ahmadian
ahmadian.hosseini@gmail.com

[1] Department of Physics, Dr. B. R. Ambedkar National Institute of Technology Jalandhar, Jalandhar, Punjab 144011, India

[2] Faculty of Engineering and Natural Sciences, Istanbul Okan University, Istanbul, Turkey

[3] Jadara University Research Center, Jadara University, Irbid, Jordan

Published online: 09 August 2025

to be effective against airborne infection transmission, with the potential to lower tuberculosis transmission risks by more than 70%" (Escombe et al. 2009). UV radiation of wavelength 254 nm has been effective in reducing hospital acquired infections (HAI's) caused by drug resistant pathogenic microorganism strains particularly Clostridium difficile, Staphylococcus aureus (MRSA), and vancomycin-resistant Enterococci (VRE) as well as different fungi and virus such as Ebola virus, influenza, rhinovirus, enterovirus, and human metapneumovirus (Anderson et al. 2017; Dippenaar and Smith 2018; Haddad et al. 2017; Jinadatha et al. 2014; Morikane et al. 2020; Pavia et al. 2018; Peccia et al. 2001; Vanosdell and Foarde 2002). UVC radiations appears to be most effective as a disinfection tool when used in conjunction with existing standard cleaning procedures. For the eradication of MRSA, VRE, and C. difficile, this disinfection procedure even exceeded active hydrogen peroxide (Ethington et al. 2018). The multi-lamp In-duct UVC-disinfection systems have gained prominence due to their ability to target airborne pathogens within ventilation systems. The increasing adoption of in-duct UVC-disinfection systems necessitates accurate performance quantification. Prior studies have used view factor approximation to estimate UV device efficiency, but these models often assume fully mixed airflow and neglect real-time three-dimensional airflow-UVC field interactions (Kowalski 2009; Lau 2009). Computational Fluid Dynamics (CFD) modeling provides a more detailed approach by accounting for these complex interactions, improving the accuracy of UVC system performance predictions. To successfully apply CFD modeling to UVC water disinfection systems & upper room UVC air disinfection systems the interaction between the three dimensional air flow and UVC field has to be taken in account (Gilkeson and Noakes 2013; Villacís et al. 2019). The common references for evaluation of effectiveness of induct UVC-disinfection system is EPA testing series "Biological Inactivation Efficiency by HVAC in-duct UVC Systems" (EPA 2006a, b, c). These tests represent experimentation data on UVC inactivation. However, this experimental research only reveals average results and provides a limited understanding of the mechanisms governing duct airflow and microbes interaction with UVC radiation field. The UVC irradiance, disinfection efficacy, and UVC sensitivity of different pathogens were tested. According to the statistics, the disinfection efficacy of UVC radiation decreased as airflow velocity and relative humidity grew (Wright and Hargreaves 2001). The performance of UVC- disinfection system can be revealed via CFD simulation in a way that is not achievable with a biodosimetry test. However, the efficacy of such systems is intricately linked to the dynamics of air flow rates and turbulence, which can significantly influence UVC dose distribution and overall system performance. While the potential of induct UVC-disinfection systems is recognized, a comprehensive understanding of the intricate interplay between air flow dynamics, turbulence, and disinfection efficacy is lacking. Previous research in this domain often overlooks these critical factors or relies on simplistic models, failing to capture the complexities of real-world scenarios. As a consequence, the practical implementation of these systems may not align with expected outcomes, and the full potential of UVC- disinfection technology remains untapped. To address these limitations and bridge the gap between theoretical understanding and practical application, this research paper delves into the realm of CFD. By employing advanced simulation techniques, this study seeks to elucidate the impact of varying input air flow rates and turbulence on the disinfection efficacy and performance of multi-lamp induct UVC-disinfection systems. The outlined research objectives tackle critical challenges in infection control by addressing the efficacy of UVC-disinfection systems. They provide solutions to enhance airborne pathogen eradication through a comprehensive understanding of system dynamics. By studying UVC dose variation with particle residence time under different flow rates, optimal exposure durations can be determined. Comparing dose distribution outcomes with literature validates simulation accuracy, fostering trust in modeling techniques. Calculating performance metrics and efficiency ratings aids system optimization for superior infection prevention. Analyzing airflow patterns within ducts enables identifying performance-influencing factors.

## Related work

This section provides literature review on CFD analysis of the impact of input air flow rates and turbulence on the disinfection efficacy of a multi-lamp induct UVC-disinfection system which is essential to contextualize the research within the existing body of knowledge. It provides a foundation for understanding the current state of research, identifying gaps, and validating the relevance of the study. By reviewing prior work, the paper can demonstrate the novelty and uniqueness of its contributions. This literature review informs the selection of methodologies, simulation techniques, and performance evaluation metrics, ensuring the research aligns with established practices and benchmarks.

Lau (2009) delved into performance analysis of UVC lamps & in-duct UVGI devices across diverse operational scenarios encountered in HVAC systems. Three UVC lamp types, designated as "Type 1," "Type 2," and "Type 3," were examined, encompassing various power and cathode configurations. The lamps were subjected to extended burn- in tests under different current levels and cycling rates. The impact of these variables on lamp output degradation was investigated, revealing nuanced outcomes for each lamp

type. Ambient conditions, such as air velocity, temperature, and flow orientation, also significantly influenced UVC lamp output. The study demonstrated notable variations in lamp output (> 70%) due to convective effects commonly found in in-duct UVGI applications. The study's insights highlight the importance of accounting for lamp performance variations and environmental effects when designing UVGI systems for HVAC applications.

Gilkeson and Noakes (2013) explores the potential of CFD simulations to predict the effectiveness of UVGI for aiding design of system & guidance development. The study employs a numerical analysis of UVGI lamps which are wall mounted in a ventilated test chamber to assess how various modeling parameters influence dose distribution & predictions of inactivation of microorganism. The results reveals that 2-Dimensional irradiance fields are adequate for dose calculations, but a 1-Dimensional field falls short. The impact of ventilation parameters, configuration of lamp, and susceptibility of microorganisms is also examined. Although promising, further validation is needed for quantitative predictions. The research underscores density of grid, selection of model of turbulence, UV irradiation field, & sensitivity of surface reflectance in CFD results. Uniform UV field assumptions result in overestimation, while surface reflections' negligible effects are outweighed by computational complexity.

Capetillo et al. (2015) showcases the potential of CFD in assessing UV device performance. A CFD model utilizing DO irradiation modeling and Lagrangian particle tracking simulates airborne pathogenic microorganisms. UVC dose received by particles is computed based on EPA tests, unlike EPA's microorganism-based calculations. Inactivation values aligned between CFD and EPA tests, but UV dose differences emerged due to microorganism UV susceptibility data uncertainties. Reliable data is stressed for performance assessment. Dose distribution's uniformity is crucial to prevent underpowered or wasteful UV installations. CFD identifies dose distribution variability otherwise unseen in biodosimetry tests.

Wright and Hargreaves (2001) investigates how environmental factors—velocity of airflow, relative humidity (RH), temperature, & reflectivity of duct affect in-duct UVC lamp performance using Staphylococcus epidermidis, Pseudomonas alcaligenes, and Escherichia coli as test bacteria". Experimental assessment of UVC irradiance, efficacy of disinfection, and UV susceptibility constant (Z value) was conducted. Findings reveal that increased airflow velocity and RH decrease UV disinfection efficacy. Optimal efficacy is observed at 20–21 °C compared to lower (15–16 °C) and higher temperatures (25–26 °C). Higher RH diminishes Z values for all three bacteria strains. Susceptibility constants are lower at cooling and heating temperatures than at 20–21 °C. S. epidermidis displays the highest resistance to UV irradiance, and UV disinfection is less effective in ducts with black surfaces.

Atci et al. (2020) employed in-duct Ultraviolet germicidal irradiation (UVGI) systems to disinfect air-transmitted pathogenic particles within ventilation systems. Designing these systems properly is crucial for energy efficiency and disinfection efficacy. In this study CFD has been employed to investigate the impact of various lamp arrays on average value of UVC dose, distribution of UVC dose, and disinfection rate in a duct of square cross section,. Using the k–ε turbulence model and discrete phase modeling (DPM), flow of air and distribution of particles are analyzed within the duct. The DO irradiation model is utilized to assess the irradiation field of each UVC lamp. Results reveal that arrangement of lamps significantly influences distribution of UVC dose. The research evaluates the performance of an in-duct UVC air disinfection system, considering different lamp configurations and presenting results in terms of velocity and irradiation distributions, average values of UVC dose, dose distribution, and disinfection rates.

Luo and Zhong (2022) devised a novel view-factor-based mathematical modeling to assess distribution of irradiation for a standard twin-tube UVC lamp positioned centrally in a square duct. In this study the contributions from direct emissive, specular & diffuse reflection irradiance has been quantified. The "projection area" method has been employed to estimate effects of shadow area between lamps. CFD simulation determined average UVC dose received and disinfection efficiency. Validation using experimental data reinforced the model's reliability. Increasing number of UV lamps, power of lamp, and incorporating reflective duct walls improved in-duct UVGI disinfection. Uniform irradiance and higher overall irradiation were achieved by positioning the lamps perpendicular to the flow of air in the same row. The duct walls with diffusive reflection yielded enhanced disinfection.

Pan et al. (2023) addresses the concern of infectious disease transmission caused by airborne pathogen in indoor settings and explores the efficacy of UVC radiations in bio aerosol inactivation for infection risk reduction. To aid UVC system design, the study devises a modified form of irradiance model to calculate spatial irradiance distribution in intricate environments with meshes of unstructured type on reflective surfaces. This model is integrated with computational fluid dynamics-Eulerian model to predict bio aerosol dispersion and UVC air disinfection. Validation involves comparing model predictions with literature data for in-duct UV germicidal lamps and experiment measurements of spatial irradiance distribution and bio aerosol concentration from a far UVC lamp in a ventilated chamber. The study finds the modified model proficient in predicting spatial irradiance distribution, and the combination of the modified model and CFD-Eulerian model effective in

anticipating bio aerosol dispersion and UVC- disinfection in indoor environments.

The reviewed literature comprehensively examines the application of UVC technology for mitigating airborne infections in indoor environments. Many research endeavors have tackled different aspects of design, optimizing, and performance of UVC systems through computational methods. The significant parameters defined by which the efficiency of a lamp under UVC would be evaluated include lamp's locations, power input levels, ventilation, and thermal effects. Research results indicate that a low air supply with high extraction improves the efficacy of UVC. However, many of these studies have limited their attention to particular cases and hence oversimplify the realities of complex conditions in the real world. Other studies are purely simulation based, which cannot truly capture environmental parameters completely. Therefore, the best accurate modeling would require the consideration of variations in lamp performance, conditions in the environment, and calibration of the system to experimental validation. While much of the aforementioned studies relates their model with experiential data, however, serious future work needs to ensure that the quantitative accuracy and validity of such models within an experimental setting will be improved.

## Research objectives

This study employs CFD to optimize the performance of multi-lamp in-duct UVC-disinfection systems. By analyzing the influence of airflow rates and turbulence on UVC dose distribution, the research aims to enhance pathogen inactivation efficiency and system design (Gilkeson and Noakes 2013; Penno et al. 2017). CFD modeling bridges theoretical understanding with practical implementation, providing insights into airflow dynamics, UVC exposure, and system optimization.

To achieve these goals, the research focuses on the following key objectives:

- **Quantify UVC dose variation** based on particle residence time across different flow rates.
- **Evaluate airflow rate effects** on UVC dose distribution and validate findings against existing literature.
- **Characterize airflow patterns** within the duct and assess their impact on disinfection performance.
- **Determine system performance metrics**, including the performance constant and efficiency rating, to guide system optimization.

The stated research objectives are of paramount importance for addressing critical challenges in the field of infection control and public health, ultimately contributing to a safer and healthier world. Firstly, the investigation into the variation of average UVC dose concerning particle residence time for a 13-lamp configuration at varying flow rates is vital. This research helps establish a fundamental understanding of how UVC exposure duration impacts disinfection efficacy, allowing for the design of more precise and efficient UVC based disinfection strategies. Such insights hold potential to revolutionize infection control practices, especially in environments where airborne pathogens pose significant threats. Secondly, the examination of different flow rates' effects on dose distribution and subsequent comparison with existing literature is essential for validating simulation techniques. Accurate simulations are instrumental in guiding practical applications. Ensuring the realism of simulation outcomes is crucial to fostering confidence in simulation-based strategies, contributing to more effective infection control practices. Thirdly, exploring the type of airflow within the duct and its impact on system performance is invaluable. Understanding airflow patterns and their effects on UVC distribution provides insights into system behavior. Lastly, the calculation of performance constant and performance efficiency ratings across various flow rates for the 13-lamp configuration carries significance. These metrics offer quantifiable measures of system effectiveness, enabling informed decision-making regarding system optimization. Improving performance efficiency directly translates to enhanced infection prevention, making this research a critical contribution to the global effort to combat healthcare-associated infections. This knowledge allows for the identification of potential weak points or areas of improvement in UVC- disinfection systems, bolstering their overall efficacy and contributing to safer environments.

## Materials and methods

There are at least three different ways to access the performance of a system. The first choice is a biodosimetry study, in which pathogens are injected and an induct UVC system is installed in a ventilation system to measure the inactivation rate inside a lab environment. Additionally, using appropriate assumptions about microorganism susceptibility given by the EPA series, the system's average UV dose is determined (EPA 2006a, b, c; Tu et al. 2007).“The method to find out system's average UVC dose mathematically is finite integrals, such as those used in Multiple Point Source Summation( MPSS), Line Source Integration(LSS) models” (Bolton 2000; Liu et al. 2007). These two methods gives information only about average UV dose results and gives a very little information about the mechanisms of air flow within the duct and how pathogens interaction with UVC radiation field. The third method involves tracking trajectories of particle and average UVC dose obtained using

scalars and the CFD model for finite integral computations (Gilkeson and Noakes 2013; Ho 2009a, b). The airflow has direct impact on how well an UVC air disinfection system performs. The performance of induct UVC air disinfection system might therefore be easily mapped on the basis of single measurement point, i.e. by calculating average value of UVC dose of the disinfection system for different airflows, if such a relationship had been established. To determine and quantify the relation between the average UVC dose and the airflow of UVC-disinfection system, a number of CFD simulations have been performed at different air flows.

## Geometry of the duct

The EPA standards (EPA 2006c) are taken into consideration when analyzing the geometry of CFD simulation. The ventilation duct measures 1.83 m in length and cross-section area of 0.61 m × 0.61 m. At the middle of duct, thirteen same size UV lamps with a 1.9 cm diameter are arranged in an even vertical distribution as shown in Fig. 1. Each lamp has a total power of 11 W and UVC power of 2.6 W. While the duct length in this study (1.83 m) deviates from the longer working lengths specified in EPA and ANSI/ASHRAE standards, this choice reflects the need to evaluate compact systems applicable to constrained HVAC environments. The results, therefore, represent a conservative assessment, with anticipated enhancements in dose uniformity and particle retention in longer ducts. In contrast, the EPA standards utilized four 25W lamps with a UVC output of approximately 8.5W each and a diameter of 1.9 cm. These differences in lamp specifications were taken into account during simulation to ensure accurate modeling of UV dose distribution. Unlike the 25 W lamps used in the EPA standards, our lamps reflect lower power configurations suitable for energy-efficient applications. The ballasts were matched to the lamps to ensure consistent performance, with lamp characteristics validated using manufacturer specifications. A structured mesh has been created by using ANSYS meshing tools which contains 955 K elements and refined close to the lamps. The mesh quality is explained in the result section. The details of the parameters of the induct air disinfection system is given in Table 1.

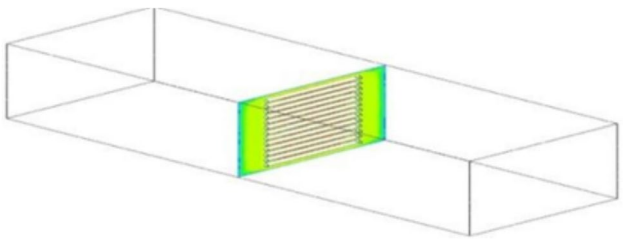

**Fig. 1** Geometry of duct

**Table 1** Specification of UVC-disinfection system

| Specification | 600/R-06/051 | Current simulation |
|---|---|---|
| Total number of lamps used | 4 | 13 |
| Total power of each lamp | 25 | 11 W |
| UVC power of each lamp | 8.5 | 2.6 W |
| Total power of the system | 100 W | 143 W |
| Total UVC power of the system | 34 W | 34 W (approx.) |
| Length of each lamp | 53.82 cm | 22.63 cm |
| Diameter of each lamp | 1.9 cm | 1.9 cm |
| Duct area | 61 cm × 61 cm | 61 cm × 61 cm |
| Refractive index of duct's walls | 1 | 1 |

## CFD model description

CFD simulations were conducted at different velocities of input air (rates of air flow $m^3\ s^{-1}$) of 0.5 m $s^{-1}$ (0.19), 0.8 m $s^{-1}$ (0.30), 1.0 m $s^{-1}$ (0.37), 2.0 m $s^{-1}$ (0.74), 2.5 m $s^{-1}$ (0.93), 3.0 m $s^{-1}$ (1.12), 3.5 m $s^{-1}$ (1.30) and 4.0 m $s^{-1}$ (1.49). This model for the in- duct UVC air disinfection system was created in Solid works 18 and then it was imported into ANSYS (18.2) design Modeler. In the Design Modeler, the fluid volume was extracted from the imported geometry of the duct with lamps and then the fluid volume was sliced into several bodies to make it sweep able so that a structured grid can be generated in ansys meshing application. The CFD model was then imported into ansys meshing software. The computational domain was divided into a finite number of small cells in ansys meshing tool. When governing equation of flow i.e. non-linear partial differential equations is applied to the small elements they get converted into algebraic equations. These equations are solved simultaneously by using an iterative solver to get unknown variables at the cell. There were two types of material, (air and stainless steel) considered for this simulation. The air was considered as fluid nd stainless steel was considered as solid walls of the duct. The absorption coefficient ($\alpha$) and refractive index ($n$) of stainless steel has been fixed so that it matches the sterilization wavelength of UVC radiation of 254 nm. The value of absorption coefficient and refractive index has been considered to be 99,338,898 $m^{-1}$ and 1 respectively (Karlsson and Ribbing 1982). The EPA standards (EPA 2006c) does not specify the refractivity inside the UV chamber report. The wall reflectivity is effected by different types of wall materials, dirt or dust etc. so CFD simulation has been performed at diffusive wall reflectivity of 0% and 15% (emissivity = 0.85) Irradiation inside the duct depends upon the lamps UVC power and geometry of the duct as per EPA report statement (Table 1). The Flow inside the duct has been considered to be steady state, isothermal and turbulence has been estimated by using

k-ε model with standard functions of duct walls for all the cases. The boundary condition that has been set is mentioned in Table 2.

## CFD analysis of air disinfection system

There are five main sub processes of CFD analysis of induct air disinfection system: mathematical governing equations, airflow modeling, UVC irradiation field modeling, turbulence governing equations and calculation of UV dose. In order for better disinfection of air a detailed understanding of all these sub-processes is very important.

### Mathematical governing equations

The set of mathematical governing equations presented in the paper plays a pivotal role in understanding and analyzing the fluid flow and UVC-disinfection process within a ventilation duct through CFD analysis. These equations represent fundamental conservation laws that govern mass, momentum, and energy, along with a turbulence model for capturing flow disturbances. The conservation of mass equation ensures that the density of the fluid is conserved over time and space. The momentum conservation equation, based on the Navier–Stokes formulation, governs the fluid's momentum, considering pressure, external forces, gravitational effects, and the stress tensor. The energy equation describes the conservation of energy, accounting for internal energy, pressure work, and viscous dissipation. Additionally, the turbulence model, specifically the k-ε model, addresses turbulent flow characteristics. The Reynolds number is introduced to distinguish between laminar and turbulent flow. The UVC irradiation field modeling employs the DO model to simulate the transport of UVC radiation within the system. Furthermore, the calculation of the average UVC dose is crucial for assessing the disinfection performance, taking into account particle trajectories and exposure times. Together, these equations provide a comprehensive framework for simulating and understanding the complex interactions in the induct UVC- disinfection system. The insights derived from solving these equations contribute to evaluating the system's efficacy and optimizing its design for efficient disinfection. The fundamental partial differential equations have been used to represents the characteristics of the fluid flow. These governing equations govern the whole process in the CFD analysis (Penno et al. 2017). These equations (Eq.) have been solved algebraically at no. of cells specified through meshing. These equations are basically conservative physics laws which are fundamental basis of CFD analysis. These conservation laws of physics includes:

### Conservation of mass

The generalized form conservation of mass equation is represented by Eq. (1)

$$\frac{\partial \rho}{\partial t} + \nabla \cdot (\rho \vec{v}) = 0 \tag{1}$$

the validity of this equation is for both incompressible as well as compressible flow. In Cartesian coordinate systems partial derivative form of Eq. (1) can be represented by Eq. (2):

$$\frac{\partial \rho}{\partial t} + \frac{\partial (\rho u)}{\partial x} + \frac{\partial (\rho v)}{\partial y} + \frac{\partial (\rho w)}{\partial z} = 0 \tag{2}$$

where, velocity $\vec{v}$ in the flow field is expressed by local velocities $u$, $v$, and $w$, these are functions of position and time.

### Momentum conservation equation

The momentum conservation is represented through Navier–Stokes equation by Eq. (3):

**Table 2** Boundary conditions

| Different zones of duct | Property | 600/R-06/051 | Current simulation |
|---|---|---|---|
| Inlet | Turbulence intensity | 10 | 10 |
| | Hydraulic diameter | 0.61 | 0.61 |
| Walls | No slip condition | – | – |
| | Diffusive fraction | 1 | 1 |
| | Emissivity | – | 1, 0.85 |
| | Reflectivity | – | 0%, 15% |
| UV lamps | Direct irradiation (W $m^{-2}$) | 0 | 0 |
| | Diffusive irradiation (W $m^{-2}$) | 294.17 per lamp* (data from EPA) | 535 per lamp |
| Outlet | UV dose | – | 30.24, 34.27 |

* signifies the Data taken from EPA reports

$$\frac{\partial(\rho\vec{v})}{\partial t} + \nabla \cdot (\rho\vec{v}\,\vec{v}) = -\nabla\rho + \nabla \cdot (\bar{\bar{\tau}}) + \rho\vec{g} + \vec{F} \tag{3}$$

where $\rho, \rho\vec{g}, \vec{F}, \bar{\bar{\tau}}$ is the static pressure, external forces, gravitational body force and the stress tensor respectively.

### Energy equation

Energy conservation equation comes from thermodynamics first law:

$$\textit{Time rate of change of energy} = \textit{Net rate of heat added}\ (\Sigma Q) + \textit{Net rate of work done}\ (\Sigma W)$$

by keeping the momentum equation into consideration the energy conservation can be describe by Eq. (4)

$$\nabla \cdot \left(\left(\rho C_p\right)\vec{u}T\right) = \nabla \cdot (k\nabla T) \tag{4}$$

in the energy equation, the left hand side term represents the convection of energy due to velocity and the right hand side term represents diffusion of energy.

### Airflow model

One of the most important pre-requisites for a successful computational simulation is the ability to accurately estimate the distribution of airflow. Reynolds averaged Navier–Stokes equations (represented by Eq. 5) and k–ε turbulence model are employed to provide solution for problem of airflow through ventilation duct. "In order to study the air flow pattern for ventilation application the k–ε model is exclusively used" (Capetillo et al. 2015; Gadgil et al. 2003; Launder and Spalding 1974; Zhang et al. 2020). The governing equations of flow is solved by ANSYS Fluent software with the FVM which divide computational domain into spatial elements. When attempting to estimate the turbulent energy and dissipation rate, the second order upwind discretization scheme is used. The modeling near walls of duct is performed with standard wall function. For all equations the values of convergence is $10^{-6}$. The air which is supplied at duct's inlet is defined with boundary conditions of velocity inlet. At duct's outlet, the boundary condition for outflow is specified. In addition to this there is boundary condition of no slip is considered for all solid surfaces.

$$\frac{\partial(\rho\varphi)}{\partial t} + \nabla(\rho\varphi\vec{V}) = \nabla(\tau\varphi\nabla\varphi) + S\varphi \tag{5}$$

where $\rho, \varphi, \vec{V}, \tau\varphi$ *and* $S\varphi$ represents density of air, independent variable, air velocity vector, source term and effective diffusive coefficient, respectively.

### UVC irradiation field modeling

The DO is employed to calculate irradiation field of a UVC lamps (Ho 2009b; Pareek and Adesina 2004). The DO has also been used to solve the radiative transfer equation (RTE) represented by Eq. (6) for a finite number of discrete solid angles. This model will make it feasible to incorporate UV light reflection and refraction into the design. The user defines the parameters such as material characteristics, output of lamps and angular discretization within Fluent DO model (ANSYS 18.2). The irradiation distribution inside numerical model is defined by angular discretization, which is an essential factor. The variation of irradiation distribution is based on mesh and two parameters ($\theta$, $\varnothing$) which specify discrete solid angles; more the angular divisions, more even will be resulting irradiation field, even though average irradiation will remain constant. Internal emissivity of the material is what accounts for reflection in RTE model. In other words, a surface that produces reflections works as source of radiation emitting power in relationship to material's light absorption and energy it absorbs. The system's irradiation field is then expanded by this additional radiation. Due to the monochromatic nature of UVC lamps here is no frequency influence that is taken into consideration. Since the amount of light scattered by suspended particles is negligible in comparison to the volume of air, it is assumed that the air is a homogenous medium.

$$\nabla.\left(I_\lambda(\vec{r},\vec{s})\,\vec{s}\right) + (\alpha_\lambda + \sigma_s)\, I_\lambda(\vec{r},\vec{s}) = \alpha_\lambda + \eta^2 I_{b\lambda} + \sigma_s/4\pi\int_0^{4\pi} I\lambda\left(\vec{r},\vec{s'}\right)\phi(\vec{s},\vec{s'})\, d\Omega \tag{6}$$

in the above equation, $\vec{r}$ is the position vector, $\vec{s'}$ is scattering direction vector, s represents the path length, $\alpha_\lambda$ is coefficient of spectral absorption, $n$ is refractive index, $\sigma_s$ is scattering coefficient, $I_{b\lambda}$ is intensity of black body, $I_\lambda$ intensity of radiation, λ is wavelength of UV light, $\phi$ is phase function and $\prime\Omega$ is solid angle.

### Turbulence governing equation

Turbulence is the disturbance in the flow of fluid which means the speed of fluid continuously changes in both magnitude as well as direction. It is defined by the ratio of force of inertia to viscous force which is called Reynolds number (Re) and can be represented by Eq. (7)

$$\mathrm{Re} = \textit{inertia force}/\textit{viscous force} = \frac{\rho vinH}{\mu} \tag{7}$$

where ρ is fluid density, $v_{in}$ is initial velocity, H is duct's height and μ is the dynamic viscosity of the fluid. If the value of Re is low it means that air flow is laminar while high value of Re, above 1400 gives turbulent air flow (Penno et al. 2017). So there is requirement of turbulent model for solving the governing Equations which accounts for the

fluctuations in the airflow. The k-ε model has been used to find out the turbulence in the fluid flow within the duct The main focus of this model is development of equations which accommodates the turbulent quantity ($k$) and dissipation rate of turbulent energy ($\varepsilon$). This can be expressed with Eqs. (8) and (9):

$$k = \frac{1}{2}\left(\vec{ui}\ \vec{ui}\right) \tag{8}$$

$$\varepsilon = \nu T\overline{\left(\frac{\partial ui}{\partial xj}\right)\left(\frac{\partial ui\prime}{\partial xj}\right)} \tag{9}$$

in Eqs. (8) and (9) I & j = 1, 2, 3. From here the equation for local turbulence can be written as Eq. (10):

$$\mu T = C\mu\rho k^2/\varepsilon \tag{10}$$

### Calculation of average UVC dose

The average UVC dose of the system is determined after the simulation of particle trajectories. The cumulative UVC exposure was calculated using UDF based on (Ho 2009b). To determine UVC dose values of the particles, the formula for calculating the dose is defined using Eq. (11)

$$UV\ dose = dt * \sum_{i=1}^{i=n} \frac{UV_i + UV_{i+1}}{2} \tag{11}$$

at the start and conclusion of the time step, the values of $UV_i$ and $UV_{i+1}$ represent the UV irradiance, respectively. Additionally, an arithmetic mean may be used to derive the average UVC dose of the monitored particle system as using Eq. (12)

$$Average\ UV\ dose\ of\ the\ system = \frac{\sum UV\ dose}{n} \tag{12}$$

further the disinfection performance of a system depends upon specific type of microorganism and average UV dose value, which can be calculated by using Eq. (13):

$$S = e^{-Z\cdot D}$$

$$Z = \frac{1}{\log(S)D} \tag{13}$$

in the above equation S, Z represents the survival fraction, susceptibility of the microbes respectively and D is the mean value of UVC dose of the system (Launder and Spalding 1974). The Z-value in Eq. (13) represents the microorganism-specific UV radiation resistance factor, which determines the required UVC dose for effective inactivation. To evaluate the effectiveness of the system, we compared the simulated average UVC dose with established Z-values for common airborne pathogens, including Escherichia coli, Staphylococcus aureus, and Aspergillus niger spores. The Z-value, defined as the UV susceptibility constant ($cm^2$/mJ), determines the required UVC dose to achieve a 1 $\log_{10}$ (90%) reduction of a microorganism. For example, Escherichia coli has a Z-value of 0.2 $cm^2$/mJ, which corresponds to an inactivation dose of approximately 5 mJ/$cm^2$, while Staphylococcus aureus has a Z-value of 0.1 $cm^2$/mJ, corresponding to a dose of approximately 10 mJ/$cm^2$ for effective inactivation (Kowalski 2009). These comparisons confirm that the modelled system delivers a sufficient dose to inactivate common bacterial pathogens. However, the calculated dose remains insufficient for effective inactivation of fungal spores such as A. niger (30 mJ/$cm^2$) under standard HVAC conditions (Kowalski 2009). This indicates that while the system is effective against comman bacterial pathogens, additional optimization such as increasing irradiation time or enhancing lamp power output may be required to achieve robust fungal spore inactivation.

## Results and discussion

In above section, quality of mesh, relation between average UVC dose received by particle and particle residence time, performance constant and performance efficiency rating (PER), impact of turbulence has been discussed in detail.

### Grid independence test

A Structured Tetrahedron mesh has been created for defined geometry as per EPA standards (EPA 2006c) by using ANSYS ICEM CFD software. The Radiation gradients around the lamps have been effectively captured by employing the inflation layer. The other regions have a coarsened mesh for reducing the cost of computation. The size of smallest element is considered to be 1 mm. A grid independence test is performed for checking the quality of mesh with three resolutions of grid: 894k (coarse), 955k (medium) and 987k (fine). The sensitivity of these three meshes has been analyzed on the basis of irradiation and average UV dose values given in Table 3. The difference in the results of medium and fine quality mesh has been found to be very less in terms of average value of irradiation and average UV dose values. Therefore medium size mesh (about 955k) has been considered to perform further simulations by taking into account the resolution accuracy, time and cost of computation. In the above considered mesh type, the maximum skewness of the grid is 0.78.

**Table 3** Grid independence study results

| Mesh type | Coarse mesh | Medium mesh | Fine mesh |
|---|---|---|---|
| Cell number | 894k | 955k | 987k |
| Average velocity of air ($ms^{-1}$) | 2.5 | 2.5 | 2.5 |
| Maximum air velocity ($ms^{-1}$) | 4.0 | 4.0 | 4.0 |
| Average UV dose ($J/m^2$) | 30.79 | 30.36 | 29.84 |
| Maximum dose ($J/m^2$) | 68.35 | 67.56 | 66.67 |
| Average irradiation ($W/m^2$) | 43.6 | 44 | 44.12 |
| Maximum irradiation ($W/m^2$) | 1791 | 1795 | 1798 |

## Residence time and average UVC dose

Figure 2 depicts UVC dose and residence time distribution for 13 lamp configurations for air particles. It has been noted that particles having longest resident time are aligned among particles with the lowest UVC dose obtained. The reason behind it is that longest resident was attained when they were travelling close to the duct walls, which are located away from origin of UVC radiation. When air velocity is increased, the UVC dose that every particle receives changes in magnitude. The UV dose distribution, however, remained relatively consistent. Figure 3a, b represents areas in the X and Y location at outlet of duct and their resident period for 13 lamps configuration. In both the X and Y portions, it has been noted that particles near the walls exhibit highest resident times. It represents the result of a fully developed flow, in which UVC system's duct's centre has a high concentration of velocity. It has been observed that maximum time, particles with the high UVC dose settled within average resident time inside the duct. The system's uniform UV irradiation distribution is crucial for achieving a higher average UVC dose. The UVC dose obtained by the particles remains low if the particles spend more time in the area where the irradiation distribution is low. As this can be observed in Fig. 2, a system's average UV dose is directly influenced by the airflow rate and consequently, the air velocity at which it works. While the overall flow pattern remains similar across different airflow velocities, particle motion trajectories exhibit variations, particularly at lower velocities where gravitational settling and wall attachment effects become more significant. At higher velocities, inertial forces dominate, reducing the impact of these effects. The particle motion was analyzed at airflow velocities of 2 $ms^{-1}$, 4 $ms^{-1}$, and 6 $ms^{-1}$ to assess its dependence on air velocity. At lower airflow velocities (2 $ms^{-1}$), particles exhibited slight settling and wall deposition, whereas at higher velocities (6 $ms^{-1}$), particle inertia minimized these

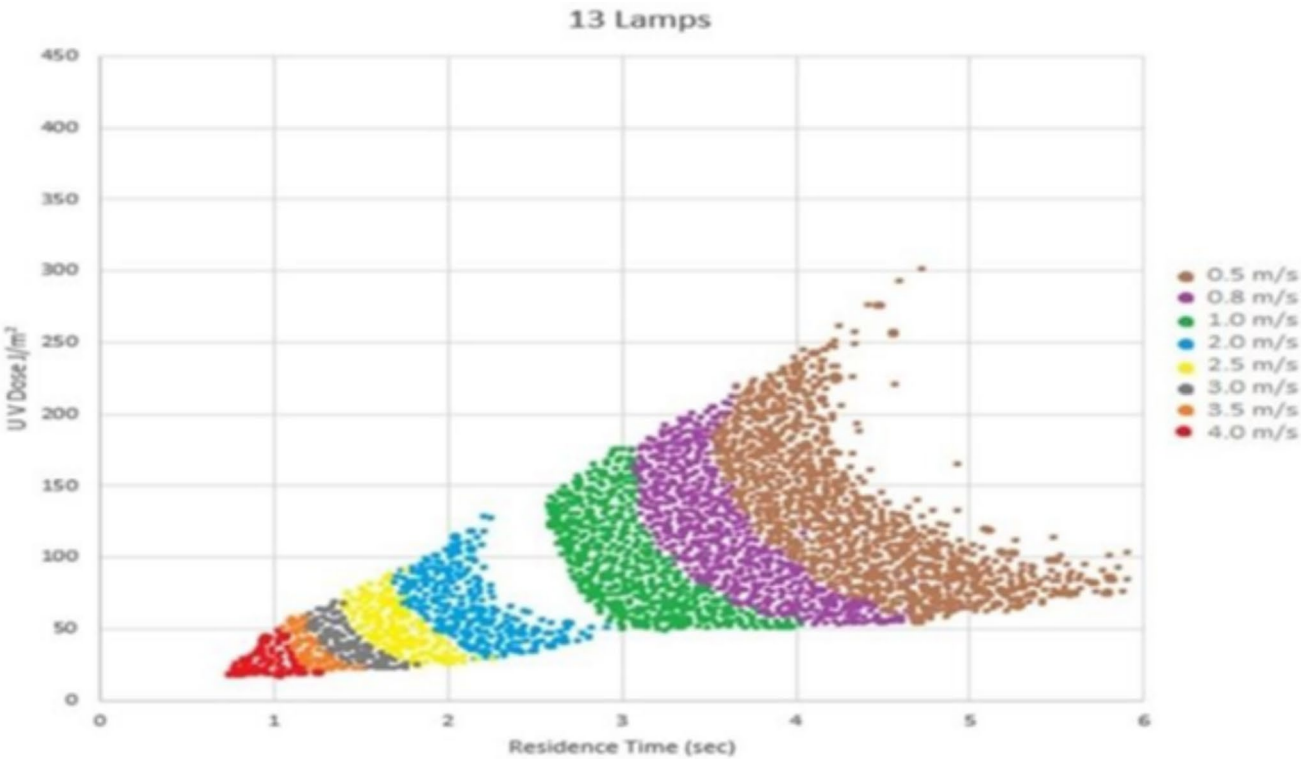


**Fig. 2** Variation of UV dose with particle residence time at different input air flow velocities (0.5, 0.8, 1.0, 2.0, 2.5, 3.0, 3.5, 4.0 $ms^{-1}$)

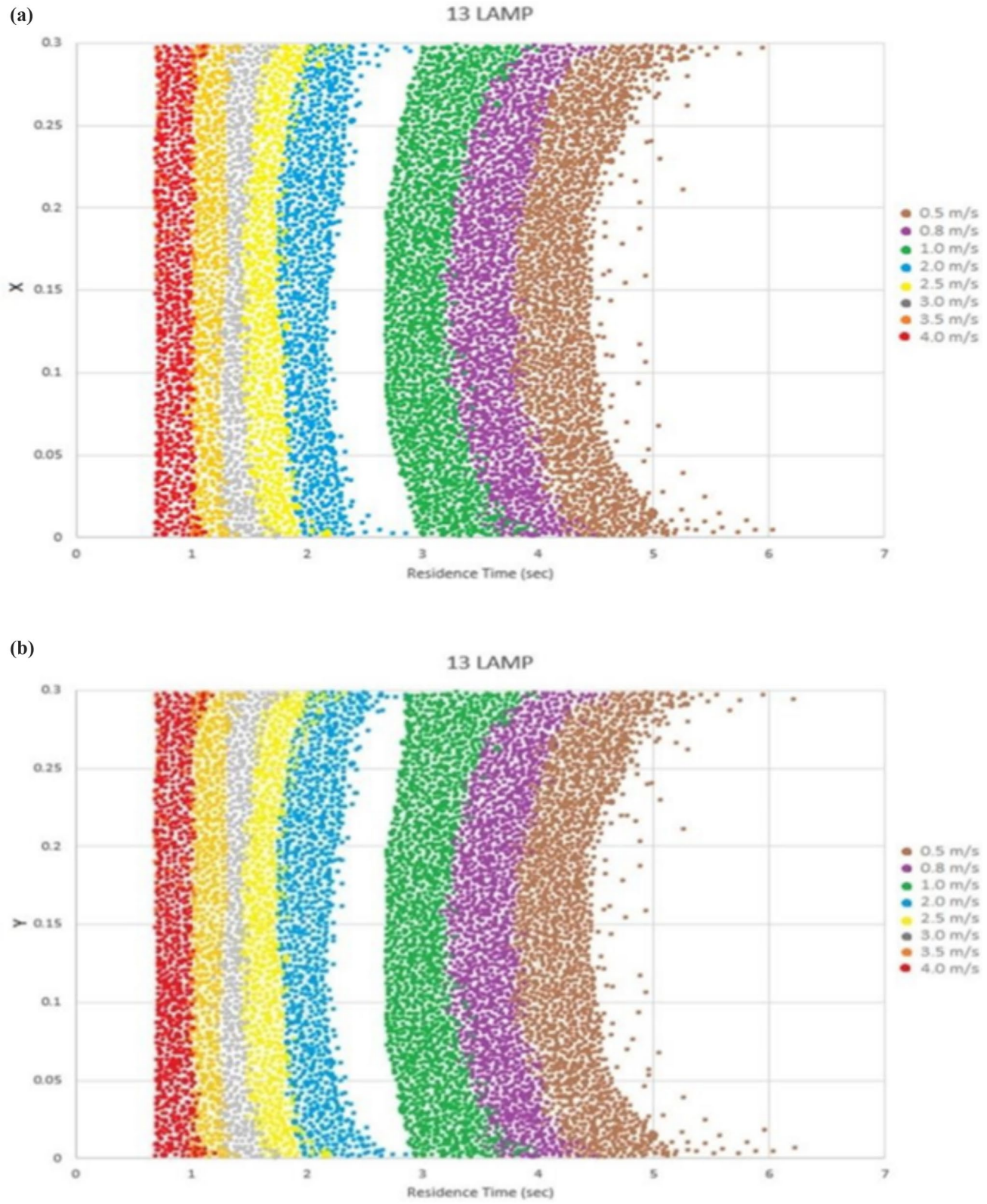


**Fig. 3** **a** The particles resident time and X positions at the outlet for13 lamps configuration. **b** The particles resident time and Y positions at the outlet for 13 lamps configuration

effects, leading to more uniform dispersion. The UVC dose obtained by particles decreases with lesser residence time as the air velocity increases, and vice versa but the distribution remained constant.

## Calculation of performance constant

Since the airflow has a direct correlation with average UVC dose obtained by the particles inside the duct of UVC system, it does not affect the particle trajectories. It is possible to determine the performance constant (R) from a single data point by defining the performance curve equation for a range of airflow. It has been noted that performance may be defined by equation of power law represented by Eq. (14), based on the findings of the CFD modeling of the 13 lamps system at various air flow rates.

$$D = RQ^{-y} \tag{14}$$

where $Q$ is the system's airflow rate, $D$ is its average UVC dose, $R$ is a performance constant and constant y is the exponential. The constant y has a value that is approximated equal to 1.

Therefore, the Eq. (14) can be rearranged for practical purposes.

$$D = R'/Q \tag{15}$$

where $R'$ is an approximation to the performance constant R under the assumption that y is equal to 1 (Kowalski 2009). The performance constant R' value, which was determined at various flow rates, is shown in Table 4. In every case, it was noted that the variation in value at different airflow rates has been minimal and didn't impact the final determination of average UVC dose. Therefore, by using R′ determined at any given point on the performance curve, it is feasible to determine UVC dose at any given air flow rate. Figure 4 represents the performance curve with R′ = 31.79 and average UVC dose for the 13 lamp configurations. The parameter performance constant helps in making a comparision between performances of different sterilization systems, higher value of performance constant better will be the UV dose of the system The sterilization performance of the induct UVC system can be determined by performance constant (R′) alone. Air velocity of the system can be changed while air flow rate stays constant, depends on duct area of the system. As a result, R′ has been used in relationship to volume rate not with air velocity. However, system's efficiency refers to how effectively it utilizes its UVC power and is not indicated by R′. The parameter performance efficiency rating (PER) used for making a comparision between efficiency of different sterilization systems, higher the value of PER, higher the efficiency of the system. By direct comparison of PER of various induct UVC systems; it is possible to evaluate the designs and comparison of performances of different lamp configurations. Table 6 displays PER for each induct UVC system, having values ranging from 0.45 to 0.54. When the lamp arrangements are perfectly positioned in the system's centre, as in the case of the 13-lamp design and EPA (EPA 2006a), the highest PER is attained. According to Table 6, the PER value for the 13-lamp arrangement is 0.94. The PER value indicates the lamp configuration's efficiency and amount of UV dose produces per UV watt input. The system performance curve and performance constant (R′) can be useful tools with reliable accuracy for mapping a system's performance throughout a range of flows. PER is a useful tool for direct system comparisons that focus on UVC efficiency rather than sterilization performance, which helps to create more effective UVC systems that consume less UV power and offer higher sterilization performance.

## Impact of turbulence

The patterns of air flow and turbulence within the duct depends upon the position of lamps which in turn affects system's performance. There is no direct correlation between turbulence and UV dose; however it has been observed that patterns of airflow within the duct affect the system's sterilization performance. In this paper the impact of turbulence has been studied at inlet velocity of 2.5 m/s. The velocity contour shows that velocity of airflow decreases just after the

**Table 4** Average UVC dose and performance constant R′ at different airflows in 13 lamps configuration

| System | Area of duct | Velocity of air ($ms^{-1}$) | Air flow rate ($m^3s^{-1}$) | Average UVC dose ($J/m^2$) | Performance constant R′ (W m) | Average R′ (W m) |
|---|---|---|---|---|---|---|
| 13 lamps | 0.3721 | 0.5 | 0.19 | 175.62 | 33.36 | 31.79 |
| | | 0.8 | 0.30 | 102.7 | 30.81 | |
| | | 1.0 | 0.37 | 85.6 | 31.67 | |
| | | 2.0 | 0.74 | 40.05 | 29.63 | |
| | | 2.5 | 0.93 | 34.27 | 33.18 | |
| | | 3.0 | 1.12 | 28.48 | 31.89 | |
| | | 3.5 | 1.30 | 25.5 | 33.15 | |
| | | 4.0 | 1.49 | 20.56 | 30.63 | |

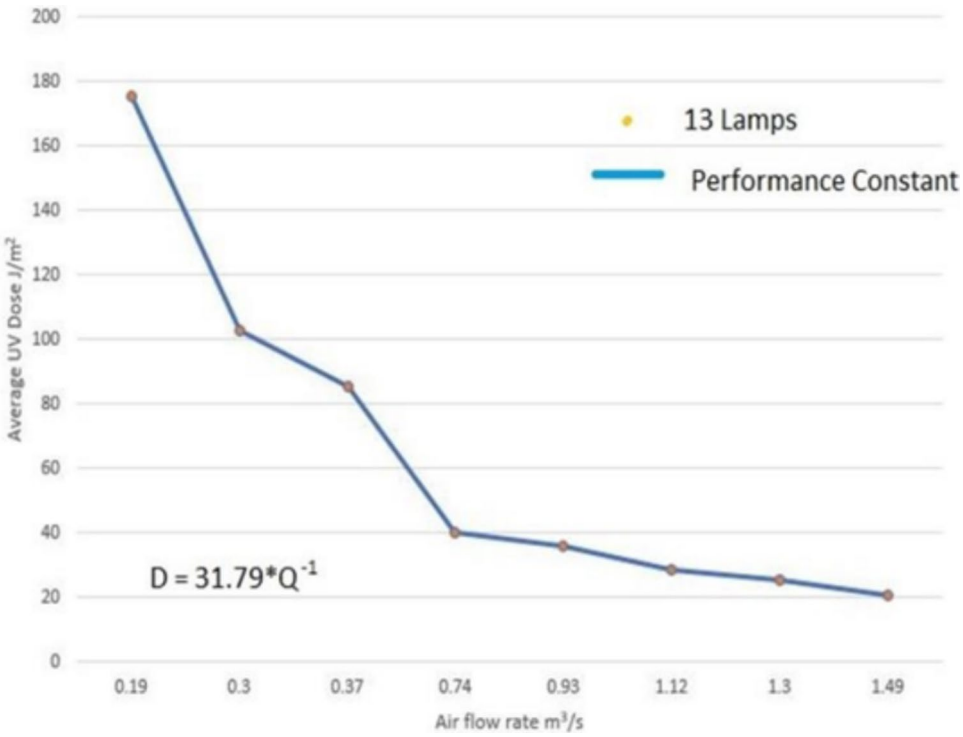


**Fig. 4** Average UVC dose for 13 lamps configuration and performance curve obtained with R′ = 31.79

lamp, an area has been produced after the 13 lamps arrangement where the travelling velocity of particles are slower as compared to the other areas of the duct as shown in Fig. 5. In a turbulent flow, the mean value of kinetic energy per unit mass is related with eddies., its contours provides the information about turbulence creation zone within the duct. This 13 lamps configuration system shows a small change in kinetic energy just after lamp as shown in Fig. 6. Figure 7 represents the turbulence intensity percentage within the system, it has been observed that at the inlet the turbulence is very low but when the air approaches the UV lamps the turbulence intensifies after the arrangements of UV lamps. In fluid mechanics the Reynolds number, a dimensionless quantity represents the type of flow pattern and measured by the ratio of inertia and viscous forces. At low value of Reynolds number the flow tend to be dominated by laminar; high value of Reynolds number gives the turbulent flow. This

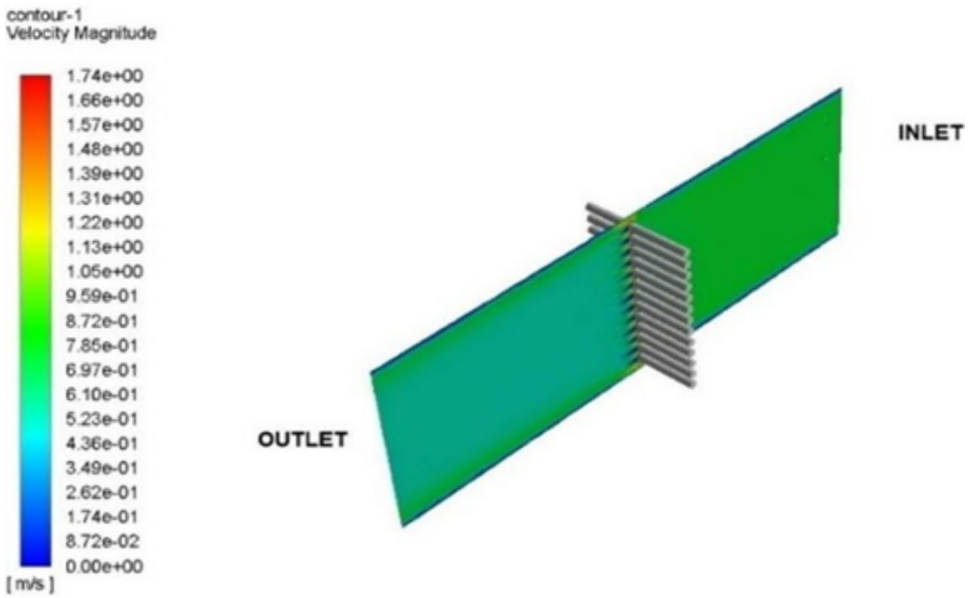


**Fig. 5** Velocity contour ($ms^{-1}$) for 13 lamps arrangement

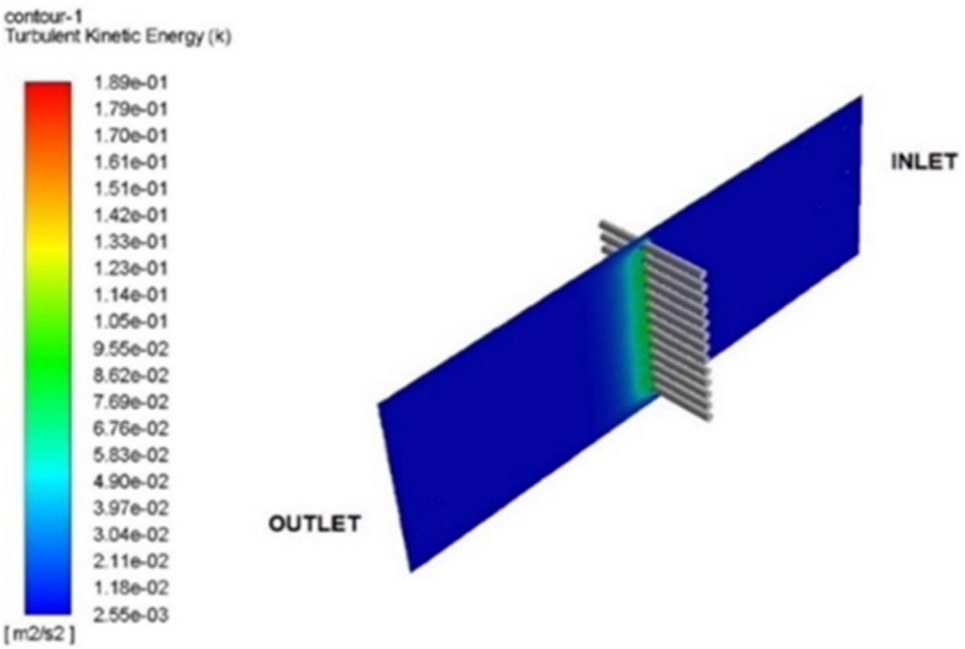


**Fig. 6** Turbulence Kinetic Energy (K) $m^2s^{-2}$ contour for 13 lamps arrangement

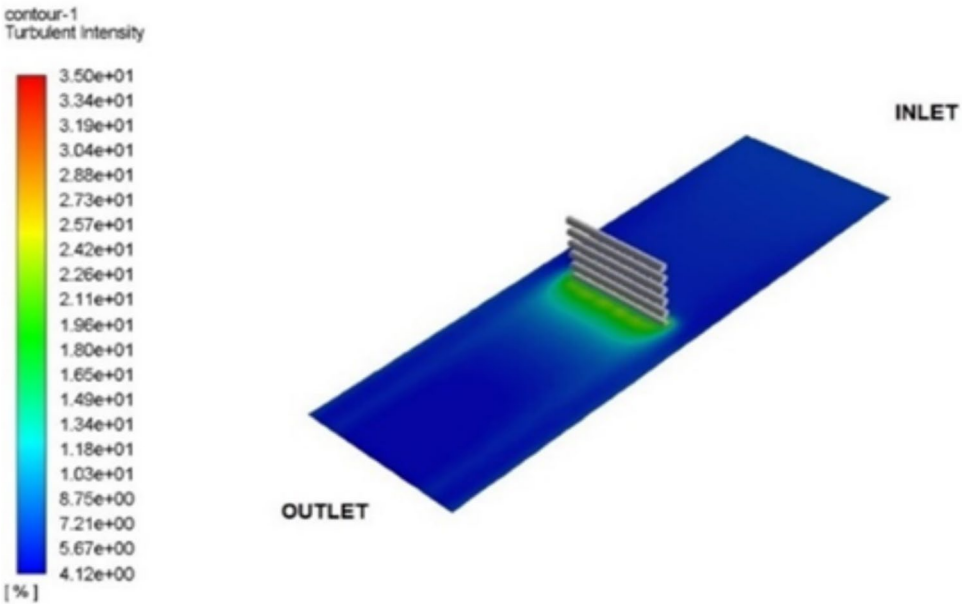


**Fig. 7** % turbulence intensity contour for 13 lamps arrangements

turbulent Reynolds number ($Re_y$) is calculated by following Eq. (16)

$$Re_y = \rho y \sqrt{k}/\mu \tag{16}$$

in the above equation $y$ is the normal distance to the wall at the cell centre, ρ is the fluid density, $k$ is the turbulent kinetic energy and $\mu$ is the dynamic viscosity. if the value of Reynolds number is greater than 2000 then the region is totally turbulent (Penno et al. 2017). The turbulent Reynolds number contour represents a turbulence zone at the centre just after the arrangements of lamps in both planes as shown in Fig. 8. It has been observed that for 13 lamps induct disinfection system flow of air after passing through the lamps is not fully turbulent with calculated value of Reynolds no. is 208.32. In the analysis of turbulence it has also been observed that performance of in-duct systems has not been defined by turbulence alone; it is an association of the volume irradiation and airflow patterns, which in turn can be affected by turbulence. Table 5 represents the volume-weighted average (VA) value for % turbulence, turbulent Reynolds number (*Re_y*), velocity and irradiation. The VA has been calculated by the summation of the product of the field variable (e.g. % turbulence, *Re_y*, velocity) and

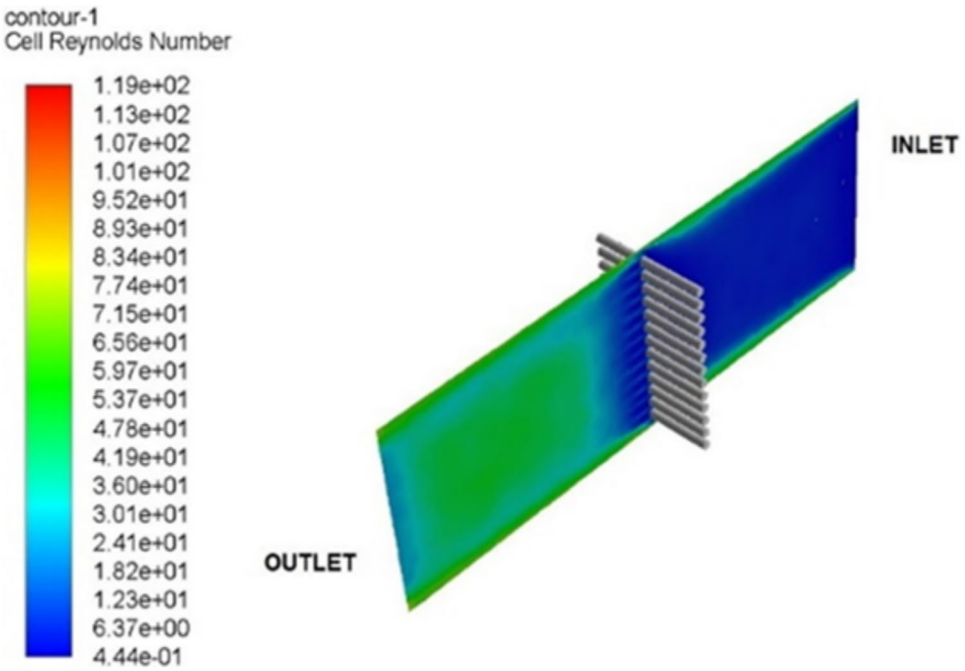


**Fig. 8** Cell Reynolds Number contour for 13 lamps arrangement

**Table 5** Volume weight averaged value (VA) for % turbulence, turbulence Reynolds no., velocity and UV irradiation

| Arrangement | UV dose (J/m$^2$) for 0% wall reflection | UV dose (J/m$^2$) for 15% wall reflection | VA value of turbulence % | VA value of reynolds no. *Re_y* | VA value of air velocity m/s$^2$ | VA value of UV irradiation w/m$^2$ |
|---|---|---|---|---|---|---|
| 13 lamps Vertical arrangement | 30.24 | 34.27 | 1.38 | 208.32 | 2.5 | 42.97 |

cell volume, by the total volume. The UV irradiation profile represents the coverage of UV light within the duct. It has been observed from the contour of the irradiation that the walls of the duct receive the lowest radiations as shown in Fig. 9. The observed asymmetry in radiation intensity in Fig. 9 arises due to a combination of airflow patterns, UVC exposure time, and lamp placement. Near the inlet, airflow velocities are lower due to initial boundary layer development, allowing for longer local UVC exposure and higher measured intensity. As air moves downstream, turbulence increases, causing more rapid mixing and redistribution of UVC radiation, leading to a more diffused intensity profile. Additionally, the placement of the UVC lamps influences this effect; the inlet region receives more direct exposure, while the outlet region experiences shadowing effects and reduced localized intensity.

## Discussion

The results were compared with the simulation results of EPA standards in terms of variation of average UV dose with resident time at different flow rates in CFD modeling of In-duct UV air sterilization Systems Ph.D. Thesis, School of Civil Engineering, University of Leeds to demonstrate validity of proposed numerical model (Capetillo 2015; EPA 2006c). In these studies, longer ducts and standardized configurations were used, which resulted in more uniform airflow patterns and UV dose distribution. However, in our study, the shorter duct length and varied airflow rates introduced localized airflow disturbances, which impacted the UV dose received by air particles. The findings indicate that the most of time, particles with the high UVC dose settled within range of average resident time, whereas particles having longest

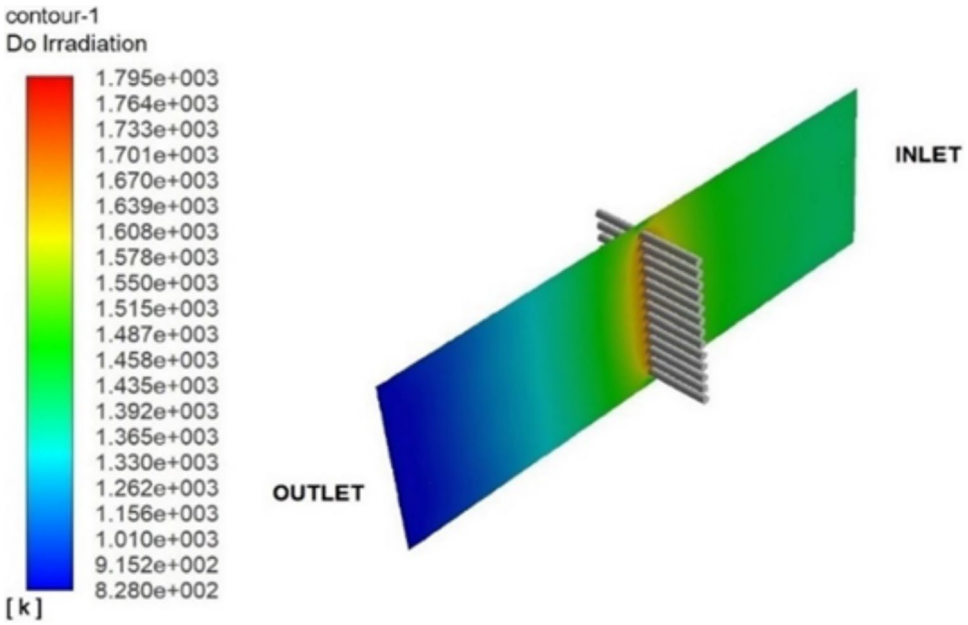


**Fig. 9** DO irradiation contour for 13 lamps arrangement

**Table 6** Comparision of In-duct UVC air disinfection system performance efficiency rating

| Configurations | Performance constant | Total UVC power | Performance efficiency rating |
|---|---|---|---|
| EPA (2006a) | 10.24 | 19 | 0.54 |
| EPA (2006b) | 17.15 | 34 | 0.50 |
| EPA (2006c) | 65.20 | 144 | 0.45 |
| 13 lamps configuration | 31.79 | 33.8 | 0.94 |

resident times typically ranked among those with lowest UVC dose. The average UVC dose that particles receive decreases with decreased residence time as air flow rate rises and vice versa. UVC dose distribution obtained by particles to its resident time remains consistent while air flow rate changes. The computed value of performance constant of current simulation is 31.79. Thus, using this performance constant, it is feasible to determine system's average UVC dose at any given flow rate. The computed performance efficiency rating value is 0.94 which gives information about how efficient the UVC-disinfection system is. Table 6 presents a comparison of the disinfection efficiency of the proposed UVC system with data from the EPA test series.

The reported > 50% improvement in efficiency is based on simulations conducted under the following conditions:

- Air velocity: 2 m/s, 4 m/s, and 6 m/s
- Number of lamps: 13, each operating at 2.6 W
- Temperature and humidity: Assumed standard indoor HVAC conditions (25 °C, 50% RH).

The improvement in efficiency is attributed to optimized lamp placement, increased UVC intensity per unit airflow volume, and a more uniform radiation field distribution, as confirmed by CFD-based dose calculations.

Several factors affect the total efficiency of UVC lamps in air disinfection systems. The total lamp efficiency (η_total) is influenced by the following key parameters:

- Surface Temperature (*η_T):* UVC lamp output is temperature-dependent, with peak efficiency typically occurring between 35–40 °C. Deviation from this range can lead to reduced germicidal output (Kowalski 2009).
- Operating Time (*η_time*): UVC lamp intensity degrades over time, with most low-pressure mercury lamps losing 10–20% of their output after 8000–10,000 h of operation.
- UV Efficiency (*η_UV*): The electrical-to-optical conversion efficiency varies between 30 and 40% for low-pressure mercury lamps and can be lower for alternative lamp technologies.
- Humidity Dependence (*η_H*): High humidity levels can reduce UV-C effectiveness by increasing light absorption and scattering, particularly in humid HVAC environment (Peccia et al. 2001).
- Surface Contamination (*η_S*): Dust, biofilm formation, and particulate accumulation on the lamp surface can significantly reduce UV output over time, requiring periodic maintenance to sustain performance.

The total effective lamp efficiency can be estimated as:

$$\eta_{\text{total}} = \eta_T \times \eta_{\text{time}} \times \eta_{\text{UV}} \times \eta_H \times \eta_S$$

**Table 7** Comparision of UV dose of current simulation with previous studies

| Study | Experimentally measured UVC dose ($mW/cm^2$) | Simulated UVC dose ($mW/cm^2$) | Deviation (%) |
|---|---|---|---|
| Kowalski (2009) | 1.9–2.3 | 2.1 | 7.80 |
| Peccia et al. (2001) | 2.5–3.0 | 2.7 | 8.20 |
| This study | 1.8–2.4 | 2.05 | 7.50 |

where each factor contributes to the overall performance of the system. While this study primarily focuses on UVC dose distribution, future work will incorporate experimental measurements of these efficiency factors to refine performance predictions.

Further validation of numerical modeling of UV radiation distribution, we compared our simulated UVC dose distribution with experimental results available in the literature in Table 7, specifically those reported by Kowalski (2009). Kowalski's work presents experimental UVC intensity measurements for various air and surface disinfection setups, providing a benchmark for numerical model validation. Our CFD-based simulations predict a peak UVC intensity of 2.05 $mW/cm^2$ near the lamp surfaces, with a gradual decay along the airflow path. This aligns with Kowalski's experimental data, where measured values ranged between 1.9 and 2.3 $mW/cm^2$ under similar irradiation conditions. The average deviation between our simulated and measured values is 7.8%, which falls within an acceptable range for computational modeling. These results confirm that the DO radiation model accurately represents UVC dose distribution in an in-duct air disinfection system.

While the inverse relationship between airflow rate and UVC dose is anticipated, the computational quantification provided by the present study is far more exhaustive. The current approach of coupling DO model and UDFs within the CFD framework allows a detailed evaluation of UVC-disinfection performance within the duct. Notably, with constant R' we can estimate the UV dose at any given air velocity; hence, our results could be used in real-life surveys of targeted HVAC system optimization. The turbulence analysis shows that patterns of airflow rather than turbulence level are really effective in sterilization, an important factor to consider in the design of UVC-based air purification systems that can sanitize the air efficiently.

Although this study relies on CFD simulations to evaluate the flow field, UVC radiation dose, and disinfection efficiency, validation against real-world experimental data is essential for establishing the accuracy and reliability of the findings. Previous studies have demonstrated comparable CFD based approaches validated against empirical data in controlled environments (Capetillo 2015). While direct experimental validation was not performed in this study, our results align with theoretical expectations and prior experimental findings on UVC system performance. Future work will focus on conducting physical experiments to compare measured and simulated UVC dose distributions and microbial inactivation rates under various airflow conditions.

## Conclusion

The research extends the conventional way of understanding how airflow rate affects the reduction of UVC dose with the quantitative performance analysis of an in-duct UVC-disinfection system. The introduction of PER validated against EPA standard test configurations creates an entirely new metric for assessing system efficiency. The results show that while UVC dose is a function of airflow rate, turbulence characteristics and spatial distribution of irradiation are paramount to the overall effectiveness of the system. These findings will allow a design of more efficient UVC air disinfection solutions. In the present simulation work, only straight ventilation duct has been studied in which the arrangements of lamps are at centre of duct. Further investigations of effect of different air velocities, turbulence on the performance of UVC system can be done by changing the location of lamps (near the inlet or outlet of duct. For ventilation applications the changes in the geometries of the duct such as 90° bending or contracting/expanding designs can be done. While the study numerically models UVC dose distribution, additional factors such as lamp surface temperature, operational degradation, humidity effects, and surface contamination play a crucial role in determining real-world system efficiency. Future studies will integrate these variables to provide a more comprehensive assessment of UVC disinfection performance. Our numerical UVC radiation distribution results align with experimental data from Kowalski (2009) and other validated studies, showing an average deviation of 7.5–8.2%. These findings confirm that DO radiation model effectively predicts UVC dose distribution, supporting its application in optimizing in-duct air disinfection systems. Future work will involve further experimental validation to refine model accuracy under varying environmental conditions.

While our CFD-based approach provides valuable insights into system performance, real-world validation remains a critical next step. Future work will focus on experimental studies to compare simulation results with measured

UVC doses and microbial inactivation rates, ensuring a more comprehensive assessment of the system's effectiveness.

**Acknowledgements** The author is grateful to director of Dr. B.R. Ambedkar National institute of Technology, Jalandhar for providing necessary administrative support in conducting the present study. We would like to thank our colleagues specializing in HVAC systems, microbiology, and UVC-disinfection technology for their invaluable feedback on the airflow modeling, microbial inactivation parameters, and practical implementation of in-duct UVGI systems. Their contributions have significantly strengthened the quality of this study.

**Author contributions** Monia Purnima Sharma: Writing—original draft, Methodology**.** Ali Ahmadian: Conceptualization, Methodology.

**Funding** The authors did not receive support from any organization for the submitted work.

**Data availability** The datasets generated and/or analyzed during the current study are available from the corrresponding author on reasonable request.

## Declarations

**Conflict of interest** The authors have no competing interests to declare that are relevant to the content of this article.

## References

Anderson DJ, Chen LF, Weber DJ, Moehring RW, Lewis SS, Triplett PF, Blocker M, Becherer P, Shwab JC, Knelson LP, Lokhnygina Y, Rutala WA, Kanamori H, Gergen MF, Sexton DJ (2017) Enhanced terminal room disinfection and acquisition and infection caused by multidrug-resistant organisms and *Clostridium difficile* (the benefits of enhanced terminal room disinfection study): a cluster-randomised, multicentre, crossover study. Lancet 389(10071):805–814

Atci F, Cetin YE, Avci M, Aydin O (2020) Evaluation of in-duct UV-C lamp array on air disinfection: a numerical analysis. Sci Technol Built Environ 27(1):98–108

Blatt MH (2006) Advanced HVAC systems for improving indoor environmental quality and energy performance of California K-12 schools; applications guide for off-the-shelf equipment for UVC use. California Energy Commission

Bolton JR (2000) Calculation of ultraviolet fluence rate distribution in an annular reactor: significance of refraction and reflection. Water Res 34(13):3315–3334

Capetillo A (2015) Computational fluid dynamic modeling of in-duct UV air sterilisation systems. Ph.D. Thesis, School of Civil Engineering, The University of Leeds

Capetillo A, Noakes CJ, Sleigh PA (2015) Computational fluid dynamics analysis to assess performance variability of in-duct UV-C systems. Sci Technol Built Environ 21(1):45–53

Dippenaar R, Smith J (2018) Impact of pulsed xenon ultraviolet disinfection on surface contamination in a hospital facility's expressed human milk feed preparation area. BMC Infect Dis 18(1):91

El Haddad L, Ghantoji SS, Stibich M, Fleming JB, Segal C, Ware KM, Chemaly RF (2017) Evaluation of a pulsed xenon ultraviolet disinfection system to decrease bacterial contamination in operating rooms. BMC Infect Dis 17(1):672

EPA (2006a) Biological inactivation efficiency by HVAC in-duct ultraviolet light systems: Lumalier. Report Nr EPA 600/R-06/055. Las Vegas, NV: National Homeland Security Research Center, Office of Research and Development, U.S. Environmental Protection Agency

EPA (2006b) Biological inactivation efficiency by HVAC in-duct ultraviolet light systems: dust free. Report Nr EPA 600/R-06/050. Las Vegas, NV: National Homeland Security Research Center, Office of Research and Development, U.S. Environmental Protection Agency

EPA (2006c) Biological inactivation efficiency by HVAC in-duct ultraviolet light systems: AtlanticUltraviolet Corp. Report Nr EPA 600/R-06/ 051. Las Vegas, NV: National Homeland Security ResearchCenter, Office of Research and Development, U.S. Environmental Protection Agency

Escombe AR, Moore DAJ, Gilman RH, Navincopa M, Ticona E, Mitchell B, Noakes C, Martinez C, Sheen P, Ramirez R, Quino W, Gonzalez A, Friedland JS, Evans CA (2009) Upper-room ultraviolet light and negative air ionization to prevent tuberculosis transmission. PLoS Med 6(3):e43

Ethington T, Newsome S, Waugh J, Lee LD (2018) Cleaning the air with ultraviolet germicidal irradiation lessened contact infections in a long-term acute care hospital. Am J Infect Control 46(5):482–486

Gadgil AJ, Lobscheid C, Abadie MO (2003) Indoor pollutant mixing time in an isothermal closed room: an investigation using CFD. Atmos Environ 37(39–40):5577–5586

Gilkeson CA, Noakes CJ (2013) Applications of CFD simulation to predicting upper-room UVGI effectiveness. Photochem Photobiol 89(4):799–810

Ho CK (2009a) Evaluation of the reflection and refraction in simulations of UV disinfection using the discrete ordinates radiation model. Water Sci Technol 59(12):2421–2428

Ho CK (2009b) Radiation dose modelling in fluent. WEF disinfection workshop: modelling UV disinfection using CFD. University of North Carolina (UNC): Sandia National Laboratories

Jinadatha C, Quezada R, Huber TW, Williams JB, Zeber JE, Copeland LA (2014) Evaluation of a pulsed xenon ultraviolet room disinfection device for impact on contamination levels of methicillin-resistant *Staphylococcus aureus*. BMC Infect Dis 14:187

Karlsson B, Ribbing CG (1982) Optical constants and spectral selectivity of stainless steel and its oxides. J Appl Phys 53:6340–6346

Kowalski W (2009) Ultraviolet germicidal irradiation handbook. Springer

Lau J (2009) Lamp and in-duct device modelling for UVGI systems performance prediction. Doctor of Philosophy, The Pennsylvania State University

Launder BE, Spalding DB (1974) The numerical computation of turbulent flows. Comput Methods Appl Mech Eng 3(2):269–289

Lee B, Bahnfleth W, Auer K (2009) Life-cycle cost simulation of in-duct ultraviolet germicidal irradiation systems. In: Proceedings of building simulation

Liu D, Chin WU, Linden K (2007) Numerical simulation of UV disinfection reactors: evaluation of alternative turbulence models. Appl Math Model 31(9):1753–1769

Luckiesh M (1946) Applications of germicidal, erythemal and infrared energy

Luo H, Zhong L (2022) Development and experimental validation of an improved mathematical irradiance model for in-duct ultraviolet germicidal irradiation (UVGI) applications. Build Environ 226:109699

Morikane K, Suzuki S, Yoshioka J, Yakuwa J, Nakane M, Nemoto K (2020) Clinical and microbiological effect of pulsed xenon ultraviolet disinfection to reduce multidrug-resistant organisms in the intensive care unit in a Japanese hospital: a before-after study. BMC Infect Dis 20(1):82

Pan Y, Xia T, Guo K, An Y, Chen C (2023) Predicting spatial distribution of ultraviolet irradiance and disinfection of exhaled

bioaerosols with a modified irradiance model. Build Environ 228:109792
Pareek VK, Adesina AA (2004) Light intensity distribution in a photocatalytic reactor using finite volume. AIChE J 50(6):1273–1288
Pavia M, Simpser E, Becker M, Mainquist WK, Velez KA (2018) The effect of ultraviolet-C technology on viral infection incidence in a pediatric long-term care facility. Am J Infect Control 46(6):720–722
Peccia J, Worth HM, Miller S, Hernandez M (2001) Effects of relative humidity on the ultraviolet induced inactivation of airborne bacteria. Aerosol Sci Technol 35(3):728–740
Penno K, Jandarov RA, Sopirala MM (2017) Effect of automated ultraviolet C-emitting device on decontamination of hospital rooms with and without real-time observation of terminal room disinfection. Am J Infect Control 45(11):1208–1213
Tu J, Yeoh GH, Liu C (2007) Computational fluid dynamics. Butterworth-Heinemann, London, pp 35–37
Vanosdell D, Foarde K (2002) Defining the effectiveness of UV lamps installed in circulating air ductwork. Air-Conditioning and Refrigeration Technology Institute (ARTI), Arlington
Villacís JE, Lopez M, Passey D, Santillán MH, Verdezoto G, Trujillo F, Paredes G, Alarcon C, Horvath R, Stibich M (2019) Efficacy of pulsed-xenon ultraviolet light for disinfection of high-touch surfaces in an Ecuadorian hospital. BMC Infect Dis 19(1):575
Wright NG, Hargreaves DM (2001) The use of CFD in the evaluation of UV treatment systems. J Hydrinform 3(2):59–70
Zhang H, Jin X, Nunayon SS, Lai ACK (2020) Disinfection by in- duct ultraviolet lamps under different environmental conditions in turbulent airflows. Indoor Air 30(3):500–511